

Embrittlement of Interfaces by Solute Segregation*

JAMES R. RICE and JIAN-SHENG WANG

Division of Applied Sciences, Harvard University, Cambridge, MA 02138 (U.S.A.)

(Received June 1, 1988)

Abstract

We discuss theoretical models of interfacial embrittlement by solute segregation. Of properties susceptible to alteration by segregation, the ideal work of interfacial separation, $2\gamma_{\text{int}}$, is predicted to have an important but probably not exclusive role in controlling embrittlement. A thermodynamic framework for estimating $2\gamma_{\text{int}}$ from data available through free surface and grain boundary adsorption studies is outlined, and relevant segregation energies are given for carbon, phosphorus, tin, antimony and sulphur segregation in iron. Data from intergranular fracture experiments involving these same segregants is also summarized in an attempt to test the idea that segregation-induced embrittlement (or ductilization) can be understood in terms of the segregant's effect on $2\gamma_{\text{int}}$. Uncertainties in present data do not allow a convincing test, but it is not implausible that the deleterious effects of phosphorus, tin, and sulphur in iron can be understood in this way. The effect of carbon does not seem to be similarly understandable, although that may be due to the inappropriateness of the only available surface segregation data in that case, which are for a (001) surface rather than a general polycrystalline surface created by intergranular fracture.

1. Introduction

Several examples are known whereby the alteration of chemical composition of grain boundaries, by the atomic-scale segregation of solutes present only as minute impurities in the bulk, causes intergranular brittleness of normally ductile solids. Examples are provided by bismuth in copper, sulphur in nickel and a range of segregants, including arsenic, oxygen, phosphorus,

tin, antimony, sulphur, tellurium and presumably hydrogen in iron [1-3]. Sometimes the presence of a segregant at grain boundaries may improve the ductility of a polycrystal that is susceptible to brittle intergranular failure. This seems to be the case for carbon in iron that has been embrittled by some of the segregants just mentioned, and also for boron in the ordered Ni_3Al alloy [4, 5].

Here we focus on the much studied cases of segregants in iron. The idea is to use the results now available from extensive experiments dealing with that case to evaluate and test theoretical concepts on interfacial cohesion, and thus to develop ideas which may find wider application to interfacial failure in other systems, including composites.

The next section examines available theory for understanding the brittle decohesion cracking of interfaces in terms of parameters susceptible to alteration by segregation. That section emphasizes the expected important, if not exclusive, role of $2\gamma_{\text{int}}$ as a controlling interfacial property in determining resistance to brittle decohesion cracking. Here $2\gamma_{\text{int}}$ is the ideal work of reversibly separating an interface against atomic cohesion. It is equal to the area under the stress σ vs. separation distance δ curve for the interface; Fig. 1.

The section which follows then reviews a thermodynamic framework which relates changes in interfacial chemical composition, due to solute segregation, to changes in $2\gamma_{\text{int}}$. The reductions (or increases) in $2\gamma_{\text{int}}$ in separations at fixed composition are shown to be related to differences between initial and final free energies of segregation. These differences are between an initial state in which the segregants are situated on unstressed interfaces, *i.e.* grain boundaries, and a final state in which they reside on the pair of free surfaces created by fracture.

Although the fractures of interest generally occur at low temperature, when the interface is out of composition equilibrium with the bulk, the

*Paper presented at the symposium on Interfacial Phenomena in Composites: Processing, Characterization, and Mechanical Properties, Newport, RI, June 1-3, 1988.

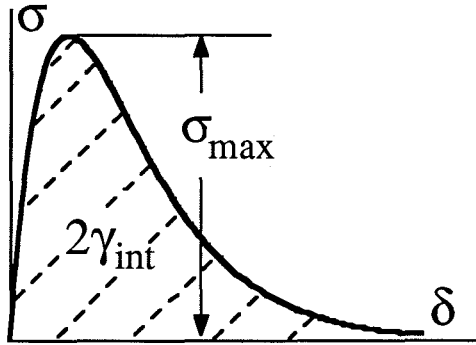


Fig. 1. Tensile stress vs. separation distance normal to an interface.

relevant free energies of segregation can be estimated from high temperature equilibrium segregation experiments. While there is substantial uncertainty and some inconsistency in reported experimental values, data exist allowing estimates of approximate ranges for the free energies both for grain boundary and free surface impurity segregation in the cases of carbon, phosphorus, tin, antimony and sulphur in α -Fe.

Thus one has the means of determining how segregation of solutes at interfaces affects $2\gamma_{\text{int}}$. The question arises: is understanding of the alteration of $2\gamma_{\text{int}}$ by solute segregation really relevant to explaining segregation-induced embrittlement in ductile or normally ductile systems, for which total works of fracture are usually much larger than $2\gamma_{\text{int}}$?

To address this we close by indicating a method of testing, with data from fracture experiments, the hypothesis that embrittlement (or ductilization) by impurity solute segregation at interfaces is explainable in terms of the effect of the segregation on $2\gamma_{\text{int}}$. The uncertainties in currently available data, both for fracture properties of solute embrittled iron alloys and for thermodynamic properties of the grain boundary and surface segregants, are so great that a convincing test of the hypothesis cannot be made at this time. The data on phosphorus, tin, antimony and sulphur in polycrystalline iron is nevertheless such that it is not implausible that their deleterious effects can be understood in terms of their alteration of $2\gamma_{\text{int}}$, which they decrease. The available data for carbon in iron do not fit the same trend, although the interpretation is unclear since a critical surface segregation energy is available only for carbon segregation on (100) planes in iron crystals rather than for general polycrystal surfaces formed by intergranular fracture.

2. Brittle decohesion cracking of interfaces

Here we briefly review theoretical models of the cracking process in order to identify material or interfacial properties relevant to crack growth resistance.

2.1. Griffith crack

In the elastic-brittle Griffith model, all plastic flow processes are neglected. The amount G per unit crack area by which the work done by external loads exceeds the change in elastic strain energy, both calculated according to continuum elasticity, is equated to the energy $2\gamma_{\text{int}}$ per unit crack area residing in the newly separated bonds. (G is proportional to the square of the stress intensity factor for the common linear elastic model of the adjoining solids; see e.g. [6].) Thus $G = 2\gamma_{\text{int}}$ for crack growth, so that the effect of alteration of interfacial chemical composition shows only through its effect on $2\gamma_{\text{int}}$ in this model. Sometimes the energy of the bonds is written

$$2\gamma_{\text{int}} = f_s^A + f_s^B - f_b^{A/B} \quad (1)$$

where A and B denote the solids that join along the interface (Fig. 2(a)) or as $2f_s - f_b$ when the solids have identical properties, where the f_s denote excess free energy per unit area for a surface (f_s) or for a grain boundary interface (f_b). A different expression, as discussed later, applies for separation of an interface in presence of a mobile segregant which can diffuse to or from the interfacial region during separation.

2.2. Cohesive zone model

This model incorporates more detail of the separation process, but does not represent the effects of atomic discreteness. In it, the interfacial region is represented as two joined elastic continua which interact with one another such that a stress vs. separation relation, $\sigma = \sigma(\delta)$ like in Fig. 1, applies along the gradually decohering interface according to the local separation δ (Fig. 2(b)). The two solids are, for the present, assumed to separate without dislocation or other inelastic processes within them and without significant shear parallel to the interface. The latter assumption may not generally be reasonable for interfaces between solids of strong dissimilarity in elastic constants, even when loaded only by tensile forces acting perpendicular to the interface (see ref. 7 and references therein). We neglect

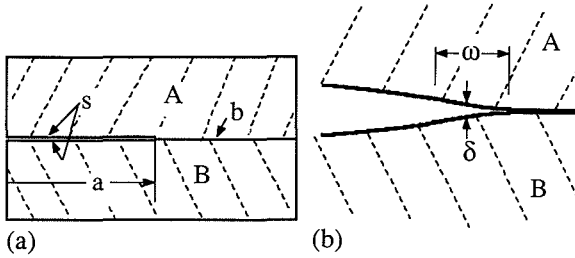


Fig. 2. (a) Interfacial elastic-brittle crack. (b) Region of gradual decohesion near tip, over size scale ω .

such effects here, although they may be important for many types of composite interfaces.

Clearly, if the interface is initially unseparated and if stressing is uniform all along it, then the failure criterion is that $\sigma = \sigma_{\max}$ of Fig. 1. However, there is a different result when the failure occurs within a transition region between a much longer crack-like zone, where the sides of the interface have been pulled out of interaction range of one another, and an also long region where the interface remains essentially unseparated, $\delta = 0$. This defines a non-singular, cohesive crack model and a well known application of the J -integral shows that the condition for crack growth reduces, in this limit, to [6, 8]

$$G = \int_0^{\infty} \sigma(\delta) d\delta \equiv 2\gamma_{\text{int}} \quad (2)$$

where G is the energy release rate for the equivalent elastic-brittle crack model, Fig. 2(a). Thus the cohesive zone model then gives complete agreement with the Griffith model.

The transition zone itself, over which the decohesion occurs, has a length ω along the interface which may be estimated from the Dugdale/BCS model. For the isotropic material of tensile modulus E and Poisson ratio ν , this gives (see, for example, [9])

$$\omega = \frac{\pi}{8(1-\nu^2)} \frac{EG}{\sigma_{\max}^2} = \frac{\pi}{4(1-\nu^2)} \frac{E\gamma_{\text{int}}}{\sigma_{\max}^2} \approx 0.9 \frac{E\gamma_{\text{int}}}{\sigma_{\max}^2} \quad (3)$$

which is a lower bound to the size since it is based on σ being uniform at σ_{\max} all along the cohesive zone. Guided by analogous discussion in [10], we shall thus estimate ω as $(1 \text{ to } 1.5) E\gamma_{\text{int}}/\sigma_{\max}^2$.

If one now assumes a σ vs. δ relation compatible with the $(1+x)e^{-x}$ type fit to the energy of the universal bonding correlation of Rose *et al.*

[11, 12] and Ferrante and Smith [13], then

$$\sigma = E_0 \left(\frac{\delta}{h} \right) \exp \left(-\alpha \frac{\delta}{h} \right) \quad (4)$$

Here h represents an unstressed separation distance between planes joining at the interface, and is of order of the atomic spacing or a little larger, and E_0 is the initial modulus for one-dimensional tensile straining of the interface layer. It then follows from $d\sigma/d\delta = 0$ that

$$\sigma_{\max} = \frac{E_0}{e\alpha} \quad (5)$$

with $\delta = h/\alpha$ at the maximum and

$$2\gamma_{\text{int}} = \int_0^{\infty} \sigma d\delta = \frac{E_0 h}{\alpha^2} \quad (6)$$

either of which determine α and, together, imply $\sigma_{\max}^2 = 2E_0\gamma_{\text{int}}/e^2 h$.

Thus the estimate of the cohesive zone ω at the crack tip as 1 to 1.5 times $E\gamma_{\text{int}}/\sigma_{\max}^2$ gives $\omega \approx (4-6)(E/E_0)h$. For the cleavage of a lattice plane, considered as an interface, $E_0 > E$ because of the Poisson effect (e.g. $E_0 = 1.35E$ when $\nu = 0.3$) and $\omega \approx 3-4$ lattice spacings. In this case the separation process may be highly localized to the crack tip and may bear little resemblance to the spread-out zone of gradual decohesion envisioned in the present model. By contrast, for a high-angle grain interface, weakened by segregation, it is plausible that h is a little larger than an atomic spacing and that the interfacial layer is elastically compliant so that $E_0 < E$. For example $(E/E_0)h = 2$ lattice spacings results in $\omega \approx 8-12$ lattice spacings. Thus weak interfaces not only require less of a stress intensity factor for elastic-brittle crack growth but also spread the decohesion zone out over a greater size scale. Both factors reduce the near-tip shear stresses generated during the separation process, and hence reduce the stresses tending to cause those dislocation processes that have been neglected in the modelling discussed thus far.

2.3. Effects of lattice discreteness

While $G = 2\gamma_{\text{int}}$ is the condition for growth of a (long) crack according to the continuum elastic models, lattice calculations are not in perfect agreement. Even when the assumed interaction potentials among the atoms is consistent with

allowing brittle decohesion of bonds along the fracture path, without nucleation of dislocations, one finds [6, 14–17] that loads corresponding to the value G^+ of the continuum G must be achieved for the onset of crack growth, and lower loads corresponding to a value G^- for the onset of healing, where

$$G^- < 2\gamma_{\text{int}} < G^+ \quad (7)$$

(The fact that $2\gamma_{\text{int}}$ must fall in the range between G^- and G^+ , as required by thermodynamics, was not recognized in some of the earlier works on the subject [16], due primarily to ambiguities in defining G so as to properly agree with that for the anisotropic elastic continuum limit of the adopted lattice model [18].)

The excess of G^+ over $2\gamma_{\text{int}}$ is referred to as lattice trapping, and it is G^+ rather than $2\gamma_{\text{int}}$ which provides the correct criterion for (non-thermally activated) crack growth. Unfortunately, it is not known in much detail how G^+ depends on the shape of the σ vs. δ relation, or on the “shape” of potentials describing interatomic interactions, and thus there is little basis for addressing how alterations of chemical composition of the interface might affect G^+ . However, with an important caveat to be discussed, recent calculations for elastic-brittle cracks in crystal lattices suggest that $G^+ - 2\gamma_{\text{int}}$ is only a small fraction of $2\gamma_{\text{int}}$, of the order of 10% or less [14, 15]. Thus, to a reasonable approximation, the effect of segregants on G^+ may be expected to be similar to their effect on $2\gamma_{\text{int}}$. Also, the difference $G^+ - 2\gamma_{\text{int}}$ is relatively small when the decohesion process is gradual, extending over many atomic spacings at the crack tip, and this is the situation to be expected with a strongly embrittled interface.

The caveat refers to the possibility [19, 20] that some incipient dislocation-like shear rearrangement of atomic bonds may occur near the crack tip in loading towards G^+ . Even if this does not involve full nucleation of a dislocation, *e.g.* with the incipient dislocation structure disappearing due to image-like attractions at the free surface after the crack grows ahead, it still might serve to make $G^+ - 2\gamma_{\text{int}}$ significantly greater than lattice calculations thus far reported have shown. As a possible example, de Cellis *et al.* [17] found an incipient twin-like shear zone in a lattice simulation of cracking of iron.

Lattice trapping effects allow the possibility of thermally activated growth, and the kinetics of

crack growth or healing must always satisfy [21]

$$(G - 2\gamma_{\text{int}})\dot{a} \geq 0 \quad (8)$$

where a = crack length. Thus $2\gamma_{\text{int}}$ is the thermodynamic threshold for growth. A similar thermodynamic restriction applies for growth in presence of a mobile solute, which can diffuse to the interfacial region during separation, or for crack growth in an environment which adsorbs onto the fresh fracture surface, provided that $2\gamma_{\text{int}}$ is appropriately re-defined using adsorption data.

2.4. Competition between cleavage and dislocation blunting

Another perspective on the effects of solute segregation on embrittlement is provided by their effect on the competition between cleaving and dislocation blunting at the tip of an atomistically sharp interfacial crack [15, 8, 22–27], Fig. 3. According to this viewpoint, an interface is regarded as intrinsically cleavable if the local stress concentration at the tip (here phrased in terms of G) necessary for cleavage decohesion, namely $G_{\text{cleave}} = G^+ \approx 2\gamma_{\text{int}}$, is less than the value G_{disl} corresponding to nucleation of a dislocation from the crack tip. Conversely, if $G_{\text{disl}} < 2\gamma_{\text{int}}$, the crack tip will first begin to blunt by dislocation emission and, presumably, a more ductile failure mode will result.

Some relevant comments on this approach are as follows [25].

(a) G_{disl} is not a fixed number for a given interface, but depends on the direction of crack growth along it [23, 25, 26], because of the different orientations of the potentially relaxing slip planes, and on the mixity of shear with tensile loading relative to the crack [15, 25]. Thus it may be the case the $G_{\text{disl}} < 2\gamma_{\text{int}}$ for some directions of cracking along a given interface, whereas

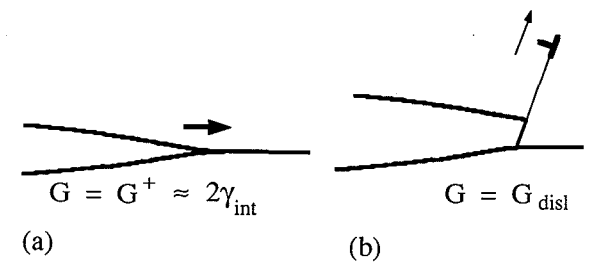


Fig. 3. Competition between (a) interfacial decohesion and (b) dislocation blunting of crack tip. System is regarded as intrinsically cleavable if G for (a) is less than for (b).

$G_{\text{disl}} > 2\gamma_{\text{int}}$ for other directions. Hence it oversimplifies to say that an interface is intrinsically cleavable. Available calculations, for that special set of cracking directions which are such that the crack tip lies in a slip plane [23, 25, 26], suggest that

$$G_{\text{disl}} = \mathcal{A}Eb^2/r_0 \quad (9)$$

where b is the Burgers vector of the relaxing dislocation, r_0 its core size, and \mathcal{A} a factor which depends on ν , the load mixity, and the particular orientation of the relaxing slip system, and which also includes a factor representing the resistance to formation of the dislocated ledge at the crack tip.

(b) Even when the intrinsic cleavability condition $G_{\text{disl}} > 2\gamma_{\text{int}}$ is met, interfaces may actually show brittleness only if there is a mechanism to nucleate the hypothesized atomistically sharp cracks, *e.g.* by stress concentrations owing to local heterogeneity of plastic flow, and if stress levels ahead of those cracks are not so much reduced by plastic flow, due to pre-existing or non-tip-nucleated dislocations, so as to cause the local crack-tip G to fall below $2\gamma_{\text{int}}$.

(c) Conversely, if the intrinsic cleavability condition is not met, in that $G_{\text{disl}} < 2\gamma_{\text{int}}$, cleavage may still occur if the mobility of tip-nucleated dislocations is sufficiently low that they cannot be driven out from the near-crack-tip region, so that stresses reaching levels of order σ_{max} , Fig. 1, develop along the interface ahead of the crack.

Thus, while the comparison of G_{disl} with $2\gamma_{\text{int}}$ in terms of the crack-tip competition provides important insight on intrinsic cleavability, the approach is not sufficient on its own to incorporate the factors mentioned in (b) and (c) which result in the strong observed dependence of brittleness on temperature and strain rate due to the dependence of plastic flow processes on those same factors. To examine the effects of alterations of composition of an interface on its intrinsic cleavability, one should therefore examine the effects on $2\gamma_{\text{int}}$ (or, more precisely, G^+) and G_{disl} . Thus if the effect of interfacial solute segregation is the typical one, of reducing $2\gamma_{\text{int}}$, this, in isolation, would make the interface more cleavable. Similarly, an effect of increasing $2\gamma_{\text{int}}$ would, in isolation, make it less cleavable. However, the segregation might also affect G_{disl} and the ease of dislocation passage through the interface, as a part of larger scale plastic stress relaxation near

the tip. For example, G_{disl} depends somewhat on the energy of the ledge left at the dislocated tip, and that is likely to have a dependence on chemical composition along the interface [24]. In addition, it has recently been observed that solutes of large atomic size relative to the host lattice, which retain some residual volume misfit even after segregating to the interface, may inhibit dislocation nucleation (*i.e.* increase G_{disl}) through an elastic interaction analogous to that in solute hardening [27]. None of these possible effects of segregation on G_{disl} and on dislocation passage through the interface can be quantified with much accuracy. Thus it is not clear if cases could exist for which, as an example, a solute segregation that decreased $2\gamma_{\text{int}}$ could have a net result of less cleavability of the interface.

2.5. Crack nucleation

In some cases interface cracks may pre-exist, but in ductile systems it is likely that most such cracks have been safely blunted in high temperature heat treatments prior to use. Thus the occurrence of interfacial fracture will require a process of crack nucleation. Sometimes this process simply occurs by the early cracking of a brittle phase, *e.g.* a carbide. Here we consider direct nucleation due to local stresses generated by the heterogeneity of flow. This is illustrated in terms of a simple dislocation pile-up in Fig. 4. It is clear that once the crack has become several atomic spacings long it is like any other interface crack and hence the controlling property is $2\gamma_{\text{int}}$, subject to the various reservations already noted. When the crack is nearer to birth, other characteristics of atomic bonding, *e.g.* as reflected in the peak strength σ_{max} and the overall shape of the σ vs. δ relation, are important too. Segregant effects that reduce σ_{max} will ease the birth of cracks at

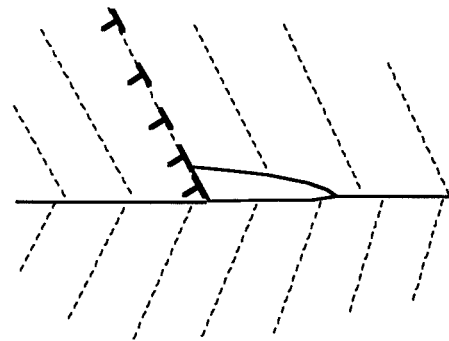


Fig. 4. Interfacial crack nucleation at a dislocation pile-up.

local stress concentrations and those that lower $2\gamma_{\text{int}}$ make it easier for them to spread to a mature size along the interface.

In the spirit of the sort of competition discussed in the last section, stress concentration at the pile-up tip may be relaxed [20] by crack nucleation or by nucleating new dislocations in the adjoining crystal and perhaps in the interface too. Segregant effects on σ_{max} and $2\gamma_{\text{int}}$ are evidently relevant to the former, it is presently unknown to what extent segregants may act to aid or inhibit the latter.

2.6. Cleavage cracking with extensive surrounding plasticity

It is normally the case in ductile systems that fractures which appear to occur by cleavage, whether of lattice planes or grain interfaces, are accompanied by significant plastic flow. Figure 5 is intended to illustrate a tensile decohesion zone that is embedded within a much larger plastic zone. The value of G , in circumstances for which the plastic zone is of small enough scale that G can be defined, is often written as

$$G = w_p + 2\gamma_{\text{int}} \quad (10)$$

where the plastic work term w_p is frequently inferred to be much greater than $2\gamma_{\text{int}}$.

For cleavage of ferrite grains adjacent to crack-nucleating carbides in steels [20] w_p is inferred to be only 1.3 to 2.5 times $2\gamma_{\text{int}}$, but it is approximately 500 to 1000 times based on G at the onset of low temperature transgranular cleavage of polycrystalline mild steel [20, 28], taking

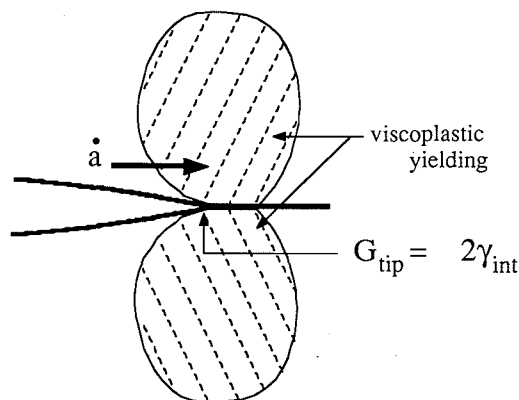


Fig. 5. Plastic/viscoplastic zone near tip of a crack growing by interfacial decohesion. In some circumstances an elastic-type stress singularity remains at a propagating crack tip, so that an energy flow to the decohesion process may be defined.

$2\gamma_{\text{int}} = 4 \text{ J m}^{-2}$ in both cases [29]. The great difference between single- and polycrystalline values has been attributed to energy absorbed in ductile tearing between the inevitably misaligned cleavage facets formed when a cleavage crack crosses a grain boundary. For cleavage of the more brittle of a suite of copper bicrystals [30] containing 0.003 at.% Bi, which segregates to and embrittles the bicrystal interface, w_p is approximately 5 times the estimated [26] $2\gamma_{\text{int}} = 2 \text{ J m}^{-2}$ for a $\Sigma 5$ symmetric tilt about [100], with (031) boundary plane, in the as-grown condition, and 25 times $2\gamma_{\text{int}}$ for a high-angle random boundary after vacuum annealing for 96 h at 723 K and some fatigue hardening. These values are based on loads on pre-cracked specimens at the onset of crack growth and might overestimate the w_p prevailing during the rapid crack propagation which followed. The same is true for polycrystalline mild steel, above. In contrast, copper bicrystals with symmetric tilt about [110], with $\Sigma 11$ ($1\bar{1}3$) or $\Sigma 9$ ($2\bar{2}1$) boundary planes, were not brittle after similar heat treatments and mechanical testing, although the latter could be embrittled by holding for 24 h in bismuth vapor at 1123 K prior to annealing for 96 h at 723 K. Presumably, w_p is a much greater multiple of $2\gamma_{\text{int}}$ for such boundaries.

Since w_p is often much larger than $2\gamma_{\text{int}}$, it is sometimes assumed that $2\gamma_{\text{int}}$ is an irrelevant parameter for such fractures. However, various authors have pointed out (e.g. [31]) that if the mechanism of fracture is, in fact, the tensile decohesion of atomic bonds, then w_p must depend in some way on the stress vs. separation curve as in Fig. 1, as well as on the plastic flow properties of the material. For example, if somehow both $2\gamma_{\text{int}}$ and σ_{max} could be reduced towards zero, it is evident that a vanishingly small stress concentration would be required at the tip for cleavage, and thus w_p would reduce towards zero too. It is not known on what features of the σ vs. δ relation w_p depends. Presumably, w_p would decrease (increase) under segregation-induced alterations of the σ vs. δ relation which decreased (increased) both $2\gamma_{\text{int}}$ or σ_{max} , but whether $2\gamma_{\text{int}}$ or σ_{max} , or something else, is the most important variable is not known in general and, probably, has no universally valid answer.

A convincing case can be made that w_p is a function only of $2\gamma_{\text{int}}$ for cleaving materials which exhibit a sufficiently strong rate sensitivity to plastic flow at high strain rates. This is rooted in

previous work of Hart [32], Hui and Riedel [33], and Lo [34], and has been developed by Freund and Hutchinson [28] and Mataga *et al.* [35]. Essentially, it is found that within a continuum plasticity formulation for a propagating, mathematically sharp-tipped crack (*i.e.* without account for a finite-sized cohesive zone), a classical inverse-square-root stress singularity of elastic type is retained at the tip, provided that the plastic constitutive response is sufficiently rate sensitive. The plastic shear strain rate $\dot{\epsilon}^p = \dot{\epsilon}^p(\tau)$ must increase with shear stress τ no more rapidly than τ^3 , *i.e.* $\dot{\epsilon}^p(\tau)/\tau^3 \rightarrow 0$ as $\tau \rightarrow \infty$, for this to occur. Since an elastic singular field is then retained at the crack tip, an energy flow to the tip, say G_{tip} , can be defined. Presuming that in Fig. 5 the actual decohesion process takes place over a size scale that is well embedded within the zone dominated by this near-tip elastic singular field, the sorts of results discussed in Sections 2.1 to 2.3 suggest that the condition for crack propagation is that

$$G_{\text{tip}} = G^+ \approx 2\gamma_{\text{int}} \quad (11)$$

Here G_{tip} is determined from the continuum plasticity analysis in terms of the history of crack growth and load variation, as well as in terms of the viscoplastic constitutive properties. For example, Freund and Hutchinson [28] and Mataga *et al.* [35] give results for the ratio G_{tip}/G as a function of crack speed \dot{a} for steady-state growth of the crack under small-scale yielding conditions such that there is net energy flux G per unit crack area. That is $G = w_p + G_{\text{tip}}$, and G corresponds to what would be called the fracture energy in such a situation. What is important for the present discussion is that the only parameter entering the fracture description that is susceptible to alteration by solute segregation is $2\gamma_{\text{int}}$, which determines the value which G_{tip} must attain for the postulated crack growth history to occur. In this model, alterations of $2\gamma_{\text{int}}$ have a “valve-like” effect on the (sometimes) much larger plastic dissipation w_p .

In other cases of crack growth with substantial plasticity, under conditions for which the very large stresses of materials with strong viscoplastic effects cannot be generated, it may be the case that σ_{max} of Fig. 1 plays a more decisive role. For example, rate-independent models of the plastic flow process lead to maximum achievable stress levels ahead of initially sharp cracks in ductile solids [36]. Under plane-strain-like constraint, a

maximum tension of about $3 \times \sigma_y$ (the tensile yield strength) results for a non-hardening material, and higher multiples of σ_y result in strain hardening materials; these factors ignore heterogeneities of the stress field at the dislocation scale, as in Fig. 4. If conditions appropriate to such rate-dependent plasticity models apply, then it would seem that cleavage of an interface would become much more difficult when σ_{max} exceeds the maximum achievable tensile stress (unless a more readily cracked brittle phase is present). Thus, in such cases, the understanding of segregation-induced alterations of σ_{max} could be critical to understanding embrittlement. Needleman [37] has developed a numerical modelling approach to interface decohesion in ductile surroundings which may be useful in assessing the effect of σ_{max} and the shape of $\sigma(\delta)$ relation.

2.7. Summary

The discussion leads us to suspect that of the parameters susceptible to change by alteration of the chemical composition of an interface, $2\gamma_{\text{int}}$ is an important parameter in determining embrittlement. The rest of the paper focuses on that parameter, but other parameters, notably σ_{max} , may also be important, and there remain possibilities that segregation might affect embrittlement by little-understood effects on dislocation generation and mobility in the immediate vicinity of the interface.

3. Interfacial decohesion in presence of a segregated solute

A thermodynamic framework [22, 38] now reviewed enables use of results from solute segregation studies to estimate effects of segregation on $2\gamma_{\text{int}}$.

With reference to Fig. 6, we focus on the interface as a thermodynamic system which is assumed to be in local equilibrium but which may be (and typically is, at low temperatures) out of composition equilibrium with adjoining bulk phases, both before and after separation. Interfacial thermodynamic quantities are defined as Gibbs-like excesses relative to those of the two adjoining phases. In defining excesses, each adjoining phase is regarded as a homogeneous system having the same mass as that phase and sustaining homogeneous deformations equivalent to those prevailing a few atomic layers away from the interface in that phase. Thus δ is defined as

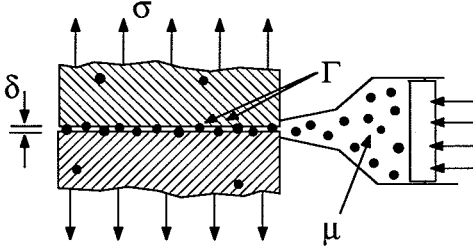


Fig. 6. Interfacial region with solute segregation, treated as a thermodynamic system that may be constrained against composition equilibrium with the adjoining bulk phase; μ is the chemical potential equilibrating solute of coverage Γ in the interfacial region.

the excess interfacial opening, *i.e.* the separation between two points, one in each of the adjoining phases, in excess of that separation which is accountable by homogeneous strain of the phases in which the two points reside. For the present discussion, the two adjoining phases are taken to be identical to one another (*e.g.* a symmetrical grain boundary) as a simplification.

We deal exclusively with solutes which are far more abundant along the interface than in a few atomic layers, well removed from the interface, in either adjoining phase. In that case Γ^i , the concentration of segregant i per unit area of interface, is well defined and we assume that an equilibrating chemical potential μ^i can be associated with each segregating species i as it exists at the interface.

Thus, where u and s are the excesses of energy and entropy per unit area of interface, in a formulation which treats the interface region as being constrained against the necessity of solute composition equilibrium with the adjoining phases, one has

$$du = T ds + \sigma d\delta + \sum_i \mu^i d\Gamma^i \quad (12)$$

for reversible changes of state. Here σ is the stress acting perpendicular to the interface and the summation extends just over the segregants. We do not consider work modes that stretch the interface in its own plane.

The key assumption, embedded in the above equation, is that all thermodynamic functions referring to the interface, *e.g.* u , s , σ and the μ^i , are determined by the values of T , δ and Γ^i , regardless of the solute concentrations (say, x_1 , x_2 , ...) in the adjoining phases. If eqn. (12) holds throughout a separation process (one in which δ

is increased towards indefinitely large values) as assumed in the present modelling, then any distinction is neglected between the pair of free surfaces resulting from such a decohesion fracture and free surfaces having the same T and Γ^i , but produced by a different thermal/mechanical route. The latter route might for instance have involved equilibrium solute segregation to the free surfaces at a higher temperature and, possibly, a surface reconstruction.

If $\delta_0 = \delta_0(T, \Gamma^1, \Gamma^2, \dots)$ is the separation for an unstressed interface (*i.e.* with $\sigma=0$) having composition $\Gamma^1, \Gamma^2, \dots$ then the work of separation is

$$2\gamma_{\text{int}} = \int_{\delta_0}^{\infty} \sigma d\delta \quad (13)$$

which is consistent with Fig. 1. This expression does not define a unique value until one characterizes the path of variation (if any) of T and the Γ^i with δ during separation. We regard T as constant during separation and thus work in terms of the excess Helmholtz function $f = u - Ts = f(\delta, \Gamma^1, \Gamma^2, \dots)$, omitting explicit reference to T as a variable. At fixed T

$$df = \sigma d\delta + \sum_i \mu^i d\Gamma^i \quad (14)$$

Thus, when there is a single segregant of amount Γ and equilibrating potential μ , one has for separation at constant Γ (the normal case at low T and with non-mobile segregants)

$$\begin{aligned} (2\gamma_{\text{int}})_{\Gamma=\text{const}} &= f(\infty, \Gamma) - f(\delta_0(\Gamma), \Gamma) \\ &= 2f_s(\Gamma/2) - f_b(\Gamma) \end{aligned} \quad (15)$$

Here $f(\infty, \Gamma) = 2f_s(\Gamma/2)$ is the free energy excess for the pair of distantly separated surfaces, so that $f_s(\Gamma/2)$ is the excess for a single one of them, where the total segregant Γ is assumed to divide equally between the two. In the usual notation, $\Gamma_s = \Gamma/2$. Also, $f(\delta_0(\Gamma), \Gamma) = f_b(\Gamma)$ refers to the unstressed grain boundary. One may then obtain the alternative expression that [22, 38]

$$(2\gamma_{\text{int}})_{\Gamma=\text{const}} = (2\gamma_{\text{int}})_0 - \int_0^{\Gamma} \{\mu_b(\Gamma) - \mu_s(\Gamma/2)\} d\Gamma \quad (16)$$

where $(2\gamma_{\text{int}})_0$ is the work to separate a clean interface (with $\Gamma=0$), $\mu_b(\Gamma)$ is the equilibrating

potential for segregant coverage Γ on an unstressed grain boundary and $\mu_s(\Gamma/2)$ for coverage $\Gamma/2$ on a single free surface.

This last equation links $2\gamma_{\text{int}}$, for separation at fixed composition, to quantities which can, in principle, be estimated from solute segregation studies. One expects that normally the potential necessary to equilibrate Γ on a grain boundary will be larger than the potential to equilibrate the same amount on a pair of free surfaces (as $\Gamma/2$ on each), $\mu_b(\Gamma) > \mu_s(\Gamma/2)$. There are, apparently, exceptions, but with this normal type of segregation behavior, the segregation reduces $2\gamma_{\text{int}}$ and thus is expected to promote embrittlement.

If $\mu = \mu(\delta, \Gamma)$ denotes the equilibrating potential for the interfacial region (with for instance $\mu(\infty, \Gamma)$ corresponding to $\mu_s(\Gamma/2)$ above), then the normal type of segregation just discussed is such that $\mu(\delta_0, \Gamma) > \mu(\infty, \Gamma)$. If, in fact, μ diminishes continuously with δ during the decohesion, such that $\partial\mu(\delta, \Gamma)/\partial\delta < 0$, then it may be proven that the peak strength σ_{max} (Fig. 1) of the interface is also reduced by segregation. This is because of the relation [22] that

$$\frac{d}{d\Gamma} \left\{ (\sigma_{\text{max}})_{\Gamma=\text{const}} \right\} = \left\{ \frac{\partial\mu(\delta, \Gamma)}{\partial\delta} \right\}_{\delta=\delta_m(\Gamma)} \quad (17)$$

where $\delta = \delta_m(\Gamma)$ is the value of δ at which the peak strength σ_{max} occurs.

For separation at constant composition in presence of multi-component segregation, the generalization of (16) is [38, 39]

$$2\gamma_{\text{int}} = (2\gamma_{\text{int}})_0 - \int_{(0,0,\dots)}^{(\Gamma^1, \Gamma^2, \dots)} \sum_i (\mu_b^i - \mu_s^i) d\Gamma^i \quad (18)$$

While separation at fixed composition seems to be the normal failure mode in low temperature embrittlement, it is useful to consider an opposite limiting case. This we consider for a single segregant of amount Γ at potential μ . This limit is separation at constant potential μ , implying that there is (for "normal" segregators) solute inflow to the interface region during separation so as to maintain μ fixed, e.g. at the value for an adjoining bulk phase with which there is composition equilibrium. Such conditions require mobility. They are probably met approximately in low temperature hydrogen assisted cracking of some interfaces (e.g. prior austenite grain boundaries in high strength quenched and tempered steels). It has been argued that they may be met also in high

temperature stress relief cracking of grain boundaries in steels due to sulphur segregation [20].

The $\Gamma = \text{constant}$ and $\mu = \text{constant}$ paths are compared in Fig. 7 which has been drawn using Langmuir-McLean adsorption isotherms (see below). For separations at fixed μ the relevant thermodynamic function is $\gamma = f - \mu\Gamma = \gamma(\delta, \mu)$, and

$$\begin{aligned} (2\gamma_{\text{int}})_{\mu=\text{const}} &= \gamma(\infty, \mu) - \gamma(\delta_0(\mu), \mu) \\ &= 2\gamma_s(\mu) - \gamma_b(\mu) \end{aligned} \quad (19)$$

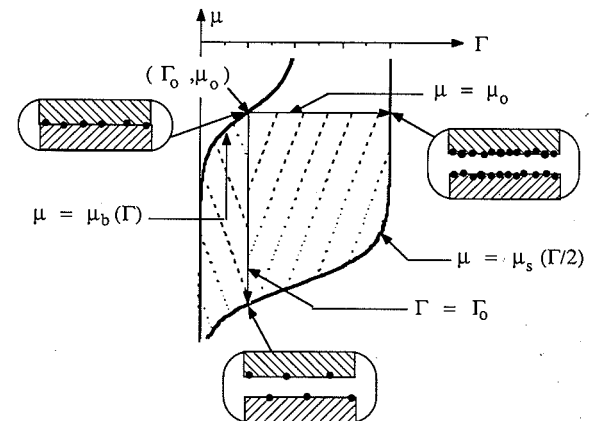
Here we have rewritten the opening of the unstressed boundary as $\delta = \delta_0(\mu)$; $\gamma_s(\mu)$ and $\gamma_b(\mu)$ denote the γ function for a single free surface and for the unstressed grain boundary, respectively. Also, it follows that [22]

$$(2\gamma_{\text{int}})_{\mu=\text{const}} = (2\gamma_{\text{int}})_0 - \int_{-\infty}^{\mu} \{2\Gamma_s(\mu) - \Gamma_b(\mu)\} d\mu \quad (20)$$

Here $\Gamma_s(\mu)$ gives the segregant coverage on a single free surface, and $\Gamma_b(\mu)$ on a grain boundary, at equilibrating potential μ .

Some relevant observations are as follows:

(1) Normal segregators have been characterized above as having $\mu_b(\Gamma) > \mu_s(\Gamma/2)$, and might analogously be expected to show $2\Gamma_s(\mu) > \Gamma_b(\mu)$. That is, at a given potential, such



Drawn for L-McL with $\Gamma_s^{\text{max}} = \Gamma_b^{\text{max}}$, $RT = 0.1$ ($\Delta g_b^0 - \Delta g_s^0$)

Fig. 7. Plots of μ vs. Γ for unstressed boundary [$\mu = \mu_b(\Gamma)$] and pair of free surfaces created by fracture [$\mu = \mu_s(\Gamma/2)$]. Paths shown for separation at constant Γ and for separation at constant μ . The μ vs. Γ plots, or adsorption isotherms, shown have been based on the Langmuir-McLean model.

segregators are situated more abundantly on a pair of free surfaces than on an unstressed grain boundary. For both separation routes considered, $2\gamma_{\text{int}}$ is reduced by such a segregator, so that they are expected to embrittle. Nevertheless, thermodynamics does not preclude the existence of anomalous segregators for which the above inequalities are reversed, *e.g.* $2\Gamma_s(\mu) < \Gamma_b(\mu)$. This means that an anomalous segregator tends to situate more abundantly on an unstressed grain boundary than on a pair of free surfaces. Such anomalous segregators increase $2\gamma_{\text{int}}$ and hence are expected to decrease interfacial brittleness. It is of interest in this regard that boron appears to be an anomalous segregator in the ordered alloy Ni_3Al , and that it reduces the severe grain boundary brittleness of that alloy [4, 5]. We discuss later the possibility that carbon may be an anomalous segregator in iron.

(2) A segregant in mobile conditions, allowing separation at constant μ , always reduces $2\gamma_{\text{int}}$ relative to the value for separation at constant Γ . That is, $2\gamma_{\text{int}}$ for "slow" separation, at fixed μ , is always less than $2\gamma_{\text{int}}$ for "fast" separation, at fixed Γ . This is because [22, 38]

$$\begin{aligned} & (2\gamma_{\text{int}})_{\Gamma=\Gamma_0} - (2\gamma_{\text{int}})_{\mu=\mu_0} \\ &= \int_{\Gamma_0}^{2\Gamma_s(\mu_0)} \{\mu_0 - \mu_s(\Gamma/2)\} d\Gamma > 0 \end{aligned} \quad (21)$$

(if $d\mu_s(\Gamma_s)/d\Gamma_s > 0$, as reasonably assumed) for paths beginning at (Γ_0, μ_0) in Fig. 7. The inequality applies for normal as well as anomalous segregators. The difference in $2\gamma_{\text{int}}$ at constant Γ compared with that at constant μ can be numerically significant, showing that mobility (or slowness of the attempted separation) is an important factor for worsening the already deleterious effect of a normal segregator on $2\gamma_{\text{int}}$, and for reducing the beneficial effect of an anomalous one. The above difference in $2\gamma_{\text{int}}$ corresponds to the cross-hatched area between the two paths in Fig. 7, whereas $(2\gamma_{\text{int}})_0 - (2\gamma_{\text{int}})_{\Gamma=\Gamma_0}$ corresponds to the cross-hatched area to the left of the $\Gamma = \Gamma_0$ path in the figure.

(3) In rapid separation at fixed composition, a thermodynamic argument drawing on the inequality nature of the second law shows that $2\gamma_{\text{int}}$ of (16) and (18) gives the least possible work to separate an interface [8]. More work could be expended if, for instance, on an atomic scale, the cracking process acted to decohere some other

set of atomic bonds than those producing the thermodynamic minimum [40].

(4) Embrittlement, at least as it mirrors $2\gamma_{\text{int}}$, is always seen to depend on differences between segregant effects on the initial grain boundary and on the two free surfaces created by the fracture. Thus a focus on the electronic alterations induced by segregants in grain boundaries, without corresponding study of what they induce on free surfaces, is unlikely to prove definitive in explaining solute embrittlement. Rather, the focus should be on the calculation of energies and entropies of segregation for both the initially coherent interface and for the surfaces created by fracture. Specifically, the differences in energy and entropy between the two states are of primary interest.

(5) When the grain boundary and surface coverages Γ entering the above formulae are less than values corresponding to full coverage of a set of adsorption sites, idealized as all having the same low energy relative to solute sites in the bulk, the simple Langmuir-McLean model [41, 42] may be adopted. Thus

$$\begin{aligned} \mu_b(\Gamma_b) &= \Delta g_b^0 + RT \ln\{\Gamma_b/(\Gamma_b^{\text{max}} - \Gamma_b)\} \\ \mu_s(\Gamma_s) &= \Delta g_s^0 + RT \ln\{\Gamma_s/(\Gamma_s^{\text{max}} - \Gamma_s)\} \end{aligned} \quad (22)$$

where the (inherently negative) Δg^0 terms are referenced to a bulk phase at the same temperature, that is they are based on the expression $\mu = RT \ln\{x/(1-x)\} \approx RT \ln x$ for the equilibrating potential when a fraction x of available solute sites are occupied in the bulk. The Δg^0 terms have the form

$$\Delta g_b^0 = \Delta h_b - T\Delta s_b^0 \quad \Delta g_s^0 = \Delta h_s - T\Delta s_s^0 \quad (23)$$

Here the Δh terms are the enthalpies of segregation (essentially identical to energies of segregation in the present context since pressure times volume terms are negligible for the unstressed boundary and free surface), and the Δs^0 terms are entropies of segregation relating to changes in the atomic vibrational spectrum. Estimated values of the Δh and Δs^0 , or of the Δg^0 at particular temperatures, are given in the next section for several segregants in iron.

Consider now a grain boundary separation at fixed composition. If the initial coverage Γ on the boundary falls within the Langmuir-McLean range, then the coverage $\Gamma/2$ on the separated surfaces is sure to do so and the equations above

for the μ can be used directly in the calculation of $2\gamma_{\text{int}}$ by eqn. (16). The integrand of (16) is then

$$\mu_b(\Gamma) - \mu_s(\Gamma/2) = (\Delta g_b^0 - \Delta g_s^0) + RT \ln \left(\frac{2\Gamma_s^{\text{max}} - \Gamma}{\Gamma_b^{\text{max}} - \Gamma} \right) \quad (24)$$

For representative boundary coverages $\Gamma = 0.25$ to $0.75\Gamma_b^{\text{max}}$, and with $\Gamma_b^{\text{max}} \approx \Gamma_s^{\text{max}}$, the last term, containing the ln, varies from 0.8 to $1.6RT$. It is $0.7RT$ when $\Gamma = 0$. Since at $T = 300$ K, typical of low temperature fractures, $RT = 2.5$ kJ mol⁻¹, and since $(\Delta g_b^0 - \Delta g_s^0)$ is of order 50 to 100 kJ mol⁻¹ (see next section) for representative embrittling solutes in iron, one is usually justified in neglecting the ln term. In that case (16) reduces to

$$2\gamma_{\text{int}} \approx (2\gamma_{\text{int}})_0 - (\Delta g_b^0 - \Delta g_s^0) \Gamma \quad (25)$$

(Since the Δg^0 have only mild temperature dependence, because representative Δs^0 vary from 0 to 0.04 kJ mol⁻¹ K⁻¹ (see next section), one might set $T = 0$ and hence write

$$2\gamma_{\text{int}} \approx (2\gamma_{\text{int}})_0 - (\Delta h_b - \Delta h_s) \Gamma \quad (26)$$

which is the form given by Rice [8]. We have a preference for (25) since it is more accurate and its terms are found by a slightly smaller range of the error-prone extrapolation in T , from a high T at which there is segregation equilibrium with solutes in the bulk.)

For multicomponent segregation within the Langmuir-McLean range, μ vs. Γ relations incorporating site competition may be assumed [42], *e.g.*

$$\mu^i(\Gamma^1, \Gamma^2, \dots) = \Delta g^{0i} + RT \ln \left\{ \frac{\Gamma^i}{\Gamma^{\text{max}} - \sum_j \Gamma^j} \right\} \quad (27)$$

Again, the last term, while decisive for high temperature equilibrium, is negligible for low temperature fracture, in which case (18) reduces to

$$2\gamma_{\text{int}} = (2\gamma_{\text{int}})_0 - \sum_i (\Delta g_b^{0i} - \Delta g_s^{0i}) \Gamma^i \quad (28)$$

4. Auger-electron-spectroscopy-based segregation energies of impurity solutes in iron

Auger electron spectroscopy (AES) has been the primary technique for recent studies of solute

segregation on grain interfaces (that can be broken open by fracture) and on the surfaces thus created. However, considerable uncertainties are introduced by the experimental conditions and assumptions which must be made in converting Auger peak height ratios, diagnostic of different solutes, into coverages Γ^i of those solutes along the boundaries under study. Quantification of the technique has not been fully developed yet. Also, there are several factors which affect the coverage of segregated atoms on an interface or exposed surface. Among them are the orientations of the interface and the surface, the composition of the examined material and the existence of other residual impurities.

The standard method of analyzing data, for a boundary or free surface thought to be in high temperature composition equilibrium with the adjoining bulk phases, is to equate μ_b or μ_s to $RT \ln x$, so that the data is represented in the Langmuir-McLean form

$$\Gamma/(\Gamma^{\text{max}} - \Gamma) = x \exp(-\Delta g^0/RT) \quad (29)$$

It is necessary to first choose a value of Γ^{max} . Then, presuming that x is known, the adopted conversion factor is used to convert the AES peak height ratio to an estimate of $\Gamma/\Gamma^{\text{max}}$. When this is done at a single temperature, the results enable calculation of a value of Δg^0 at that temperature for the data to be represented by (29). When results are obtained over a range of temperature, the procedure is to extract a Δh and Δs^0 which enable the best representation of the results over that range with $\Delta g^0 = \Delta h - T\Delta s^0$.

This is the route to the values of Δh , Δs^0 or Δg^0 that we list shortly. However, it is well to recognize that the concept of the segregation energy, particularly on a polycrystal surface, is only a macroscopic average based on the Langmuir-McLean segregation law. Atomistic calculations show that even for a single macroscopically planar interface, the bonding energy of a segregant atom may change from site to site. There is no unique segregation energy, and even on the average, the Langmuir-McLean equation is not always valid. Keeping all this in mind, one is not too surprised at the large scatter of the available data.

AES-based (mostly) segregation data in iron are listed in Table 1 for that set of impurity solutes for which results are available constraining, somewhat, both grain boundary and free surface segregation energies, so that eqns. (25)

TABLE 1 AES-based surface and grain boundary segregation data in iron (in kJ mol⁻¹)

Impurity	Segregation point	$-\Delta g_{s/b}^0$ (at T)	$-\Delta h_{s/b}$	$\Delta s_{s/b}^0 \times 1K$	Reference	
C	(100) surface		84	± 0.004	Grabke [55, 56]	
	Grain boundary		57	0.022	Grabke [55, 56]	
				38	0.043	Hänsel and Grabke [43]
				79 ^a	-0.013^a	Papazian <i>et al.</i> [65]
Sn	Polycrystal surface	77 (823 K)	46	0.045 ^b	Seah and Lea [61]	
	Low-index surface		> 200		Grabke [55]	
	Grain boundary	45 (823 K)	13	0.045 ^b	Seah and Lea [61]	
23			0.026	Grabke [55]		
P	Polycrystal surface	> 80 (973 K)			Guttman [63]	
	Low-index surface ^c		75		Grabke [56]	
				180 ^c		Grabke [55]
	Grain boundary		34	0.022	Grabke [55, 56]	
			32	0.022	Guttman <i>et al.</i> [52]	
			21	0.037	Hänsel and Grabke [43]	
Sb	Polycrystal surface	> 105 (1023 K)			Dumoulin <i>et al.</i> [64]	
	Grain boundary	20–40 (1023 K)			Guttman [66]	
13 ^d				Guttman [67]		
S	Polycrystal surface		165		Tauber and Grabke [57]	
			190		Grabke [56]	
	Grain boundary	75 (1143 K)			Suzuki <i>et al.</i> [47]	

^aAutoradiography data.

^bBased on assumed entropy expression by Seah and Lea [61], evaluated at 823 K.

^cApparently for low-index crystal surface; data and details of study unpublished.

^dRutherford back scattering spectroscopy data.

and (28) can be applied. The elements for which such are currently available are carbon, phosphorus, tin, antimony and sulphur. The uncertainties are seen to be sufficiently large that sometimes data obtained by the same research group scatter widely. Based on these data we estimate values of $\Delta g_b^0 - \Delta g_s^0$ at $T = 300$ K. These will be used in the next section in a comparison with fracture data.

We start with carbon. Carbon is known as a grain boundary cohesion enhancer in steels [43–48]. It has been confirmed that the role of carbon in improving ductility of iron alloys and steels is two-fold. One effect is to displace harmful impurities, such as phosphorus [43, 46, 49–54], tin [55], and sulphur [47, 56–58] from grain boundaries and thus reduce the detrimental effects of these impurities. Carbon is thought to be effective in this way due to its unusually large value of $-\Delta g_b^0$, compared to other segregants, which favors it in site competition. The other effect is an inherent one in that carbon itself increases the grain boundary cohesion. To obtain reliable AES data for carbon is a very difficult

task since the exposed surface of the specimen is easily contaminated by carbon even in an extra-high-vacuum AES chamber.

The only available value for surface segregation of carbon was measured on the (100) crystallographic plane, and gives $-\Delta h_s = 84$ kJ mol⁻¹. There are reasons to suspect that this value may be too high to be representative of polycrystalline surfaces created by intergranular fracture. First, since carbon can be displaced from an iron surface by tin [59], one expects $-\Delta h_s^C$ to be less than $-\Delta h_s^{Sn}$ (strictly, $-\Delta g_s^{OC}$ should be less than $-\Delta g_s^{OSn}$ at the displacement temperature). The values reported in Table 1 do not support this. Thus we have reinterpreted the 84 kJ mol⁻¹ for $-\Delta h_s^C$ as the upper limit of a possible range, 74–84 kJ mol⁻¹, with a corresponding range allowed later for tin. Second, since the 84 kJ mol⁻¹ is for a (100) crystal surface, it is well to observe that with phosphorus and tin, for which segregation energies have been estimated both for low-index crystal surfaces and for polycrystal surfaces, the low-index surface values are considerably higher than those for polycrystal surfaces

(Table 1). A low energy electron diffraction study [60] showed that the segregated carbon atoms sit in octahedral sites on the (100) plane as interstitials. For an average polycrystal surface the number of this type of interstitial site is less than on a {100} plane, and it is expected that the surface segregation enthalpy for non-(100) planes might be lower than the range of $-\Delta h_s = 74-84$ kJ mol⁻¹. However, based on that range and other data listed in Table 1, *e.g.* for grain boundaries, a range of $\Delta g_b^0 - \Delta g_s^0$ for carbon at 300 K is estimated to be -2 to 35 kJ mol⁻¹. The lower end of this range is based on the Δh_h^c from autoradiography measurements; AES results support the upper end. If $-\Delta h_s^c$ has been overestimated as discussed above, then the difference $\Delta g_b^0 - \Delta g_s^0$ could take more strongly negative values, consistent with carbon acting to increase $2\gamma_{\text{int}}$.

The segregation of tin on iron surfaces was studied by Rösenberg and Viefhaus [59] on (100), (110) and (111) crystallographic planes of Fe-4wt.%Sn alloy single crystals and by Seah and Lea [61] on polycrystal surfaces of Fe-Sn alloys with much lower tin concentrations (0.001-1.0 wt.% Sn). It was found that an order-disorder transition occurred at high coverage leading to a multilayer segregation, and the Langmuir-McLean type segregation law is then invalid. No unique segregation enthalpy and entropy could be derived. Based on the fact that even at low bulk concentration saturated structures were always observed, Grabke [55] estimated that the enthalpy for surface segregation of tin on the low-index crystal surfaces mentioned must be relatively high, $-\Delta h_s \geq 200$ kJ mol⁻¹. Considering that tin can be displaced by sulphur from the iron surface when the bulk concentration of sulphur is much lower than that of tin [61, 62], this value of $-\Delta h_s$ is far too high to be representative of polycrystalline surfaces. Seah and Lea [61] obtained a much lower polycrystal value of $-\Delta h_s = 46$ kJ mol⁻¹ (based on a polycrystalline value of $-\Delta g_s^0 = 77$ kJ mol⁻¹ at 823 K; from this they inferred, based on an assumed form for Δs^0 (giving 0.045 kJ mol⁻¹ K⁻¹ at 823 K), that $-\Delta h_s = 46$ kJ mol⁻¹). Lea and Seah [62] found that multilayer segregation would not occur if the bulk concentration is lower than 0.005 wt.%. As an impurity in steels this condition is usually satisfied and Seah and Lea's value for Δg_s^0 might be appropriate. Considering that tin can displace carbon from iron surfaces, this value is taken as

the lower limit and a range $-\Delta g_s^0 = 77-87$ kJ mol⁻¹ at 823 K is assumed. Also, assuming what seems to be a more typical $\Delta s_s^0 = 0-0.03$ kJ mol⁻¹ K⁻¹ and $\Delta s_b^0 = 0.02-0.03$ kJ mol⁻¹ K⁻¹, to extrapolate in T , rather than the larger values of Seah and Lea, a range of $\Delta g_b^0 - \Delta g_s^0$ at 300 K for tin of $26-57$ kJ mol⁻¹ is estimated.

Grabke [55, 56] reported two contrasting values of segregation enthalpy of phosphorus on iron surfaces, $-\Delta h_s = 75$ kJ mol⁻¹ as a polycrystal value and what, from context, appears to be a low-index crystal surface value of 180 kJ mol⁻¹. Details and supporting data for the latter are unpublished. Guttmann [63] gave $-\Delta g_s^0 > 80$ kJ mol⁻¹ at 973 K. We interpret this as $80-90$ kJ mol⁻¹ and selecting Δs_s^0 as $0.01-0.03$ kJ mol⁻¹ K⁻¹ gives a $-\Delta h_s$ approximately consistent with the 75 kJ mol⁻¹ noted above. Thus we estimate a range of $\Delta g_b^0 - \Delta g_s^0$ at 300 K for phosphorus of $35-48$ kJ mol⁻¹.

Segregation of antimony has been less investigated. Dumoulin and Guttmann [64] showed that in Fe-Sb alloys with 0.06 at.% Sb an equilibrium surface segregation could be reached with the saturation level less than 1 monolayer and the segregation process could be described in the framework of the Langmuir-McLean theory below 973 K when the evaporation rate is very low. The surface segregation energy was estimated only as $-\Delta g_s^0 > 105$ kJ mol⁻¹ at 1023 K. We interpret this as $105-130$ kJ mol⁻¹. Using the estimated values of $\Delta s_s^0 = 0-0.03$ and $\Delta s_b^0 = 0.02-0.03$ kJ mol⁻¹ K⁻¹, we estimate $\Delta g_b^0 - \Delta g_s^0 = 58-122$ kJ mol⁻¹ at 300 K for antimony.

It has been known that sulphur is of strong embrittlement potential if manganese does not exist [56]. Sulphur is most susceptible to surface segregation. The polycrystalline surface segregation enthalpy, $-\Delta h_s^0$, was reported to be 165 kJ mol⁻¹ [57] and 190 kJ mol⁻¹ [55]. Ignoring the modest entropy corrections for the surface segregation, in view of this range, and assuming $\Delta s_b^0 = 0.02$ kJ mol⁻¹ K⁻¹, we estimate $\Delta g_b^0 - \Delta g_s^0 = 107-140$ kJ mol⁻¹ at 300 K for sulphur.

The estimated data for the Δg^0 quantities at 300 K for carbon, tin, phosphorus, antimony and sulphur are summarized in Table 2. Also shown is a measured of embrittlement sensitivity, to be discussed in the next section.

To understand the order of the reduction of $2\gamma_{\text{int}}$ that is implied by the results just summar-

TABLE 2 Summary of ranges of Δg_s^0 at 300 K (in kJ mol⁻¹) and embrittlement sensitivities, ξ (in K/at.% in g.b.)

Impurity	$-\Delta g_s^0$	$-\Delta g_b^0$	$\Delta g_b^0 - \Delta g_s^0$	ξ
C	73-85	50-75	-2-35	-20-10
Sn	61-87	30-35	26-57	15-38
P	76-80	32-41	35-48	5-20
Sb	83-130	8-25	58-122	28-67
S	165-190	50-58	107-140	35-45

To get $-\Delta h_s$, decrease $-\Delta g_s^0$ by approximately 0 to 9; to get $-\Delta h_b$, decrease $-\Delta g_b^0$ by approximately 6 to 9.

ized, we may note that $\Delta g_b^0 - \Delta g_s^0 = 50$ to 100 kJ mol⁻¹ is representative for deleterious segregants in Table 2. If we consider a grain boundary with a square network of possible adsorption sites, spaced 0.25 nm from one another, and suppose that only one quarter of these are taken by the segregant, then $\Gamma = 4 \times 10^{18} \text{ m}^{-2} = 7 \times 10^{-6} \text{ mol m}^{-2}$. Thus for separation at this composition

$$2\gamma_{\text{int}} \approx (2\gamma_{\text{int}})_0 - (0.35 \text{ to } 0.70) \text{ J m}^{-2} \quad (30)$$

Since $(2\gamma_{\text{int}})_0 \approx 3.1 \text{ J m}^{-2}$ for a typical boundary in pure iron [29], this is a significant alteration.

The reductions from $(2\gamma_{\text{int}})_0$ will be yet greater when conditions of mobility allow separation at constant μ . Typically, in that case the surface ends up fully covered (Fig. 7) according to the Langmuir-McLean model for surface segregation, which means that the Langmuir-McLean model will not necessarily apply and, instead, multilayer coverage may occur. However, from the geometry of Fig. 7, we may expect that a calculation based on (20) with Langmuir-McLean for the surface could only underestimate the reductions of $2\gamma_{\text{int}}$ that would be calculated from the actual surface adsorption isotherm, since $\mu \rightarrow \infty$ as $\Gamma \rightarrow 2\Gamma_s^{\text{max}}$ in the Langmuir-McLean model, so we proceed on that basis. Assume then, that $\Gamma_s^{\text{max}} = \Gamma_b^{\text{max}}$ both correspond to coverage of half the network of adsorption sites mentioned above, and that the segregation energy difference is large compared with RT . As a specific illustration, assume that the fixed μ at which the separation is imagined to occur is such as to equilibrate $\Gamma = 0.5 \Gamma_b^{\text{max}}$ (*i.e.* a quarter of the network of sites covered) on the unstressed boundary. This is the case illustrated in Fig. 7. Then the reduction from $(2\gamma_{\text{int}})_0$ is approximately four times that in the previous example for separation at constant Γ . That is the reduction would range from 1.4 to 2.8 J M⁻² in the imagined separation at constant μ , which is

substantial but possibly underestimates the actual effect.

5. Fracture tests and embrittlement sensitivities

There do not seem to exist results of fracture experiments which would enable a careful test of the degree to which alterations of $2\gamma_{\text{int}}$ control solute embrittlement. What is widely available is the characterization of segregant effects on the ductile-brittle transition temperature (DBTT) in the Charpy impact test of iron and steels. Here the concern is with a low temperature brittle mode that involves intergranular fracture, or some mixture of it with transgranular cleavage, that transitions into a ductile tearing mode of rupture with increase of temperature. Most commonly, these effects have been reported as a variation $\delta(\text{DBTT})$ in DBTT associated with variations $\delta\Gamma^i$ in solute coverages, under conditions for which microstructural dimensions and plastic flow resistance (in practical terms, as measured by hardness at a given temperature) are held constant. This correlation has been reported extensively as the linear form

$$\delta(\text{DBTT}) = \sum_i \xi_i \delta\Gamma^i \quad (31)$$

where the constants ξ_i are called embrittlement sensitivities.

We give values, or approximate ranges, of the ξ_i later. The most reliable values of the Γ^i are determined by AES measurements on the intergranular fracture surface, as discussed earlier. Unfortunately, there are several possible definitions of the DBTT, *e.g.* as the temperature at which (a) the Charpy energy exceeds some fixed value (say, 2.7 J), or (b) the energy is half way between its upper and lower shelf values, or (c) the fracture surface area is of half intergranular (possibly with transgranular) cleavage and half ductile rupture appearance.

In principle, if the uncertainties in all quantities concerned were not so large, the values of the ξ_i could be used to test the hypothesis that $2\gamma_{\text{int}}$ controls interfacial embrittlement. We recognize that if the hypothesis is correct, then

$$\text{DBTT} = F(2\gamma_{\text{int}}, \text{microstructure}) \quad (32)$$

That is, solute segregation influences DBTT only through its effect on $2\gamma_{\text{int}}$, under conditions as assumed above for which "microstructure" (*i.e.*

microstructural dimensions and parameters like dislocation density and entanglements determining plastic flow resistance) are unaffected by the segregation treatment.

Current theory is, of course, unable to predict the above function F but, if it exists, then

$$\delta(\text{DBTT}) = \frac{\partial F}{\partial(2\gamma_{\text{int}})} \delta(2\gamma_{\text{int}}) \quad (33)$$

in alterations of the material which leave microstructural dimensions and plastic flow resistance unchanged. In the sub-monolayer coverage range for which the linear form of (31) is contemplated, one can use (28) and thus write

$$\begin{aligned} \delta(2\gamma_{\text{int}}) &= \sum_i [\partial(2\gamma_{\text{int}})/\partial\Gamma^i] \delta\Gamma^i + [\partial(2\gamma_{\text{int}})/\partial T] \delta T \\ &= -\sum_i (\Delta g_b^{0i} - \Delta g_s^{0i}) \delta\Gamma^i - 2s_{\text{int}} \delta(\text{DBTT}) \end{aligned} \quad (34)$$

where $2s_{\text{int}} = -\partial(2\gamma_{\text{int}})/\partial T$ at fixed composition. The second term on the right above arises because of the temperature dependence of $2\gamma_{\text{int}}$; eqn. (32) is actually an implicit equation for DBTT since $2\gamma_{\text{int}}$ depends not only on the Γ^i but also on T (=DBTT, for the purposes of that equation).

Thus, if the hypothesis is correct that solute effects are to be understood solely through effects of segregation on $2\gamma_{\text{int}}$, then from the last two equations

$$\delta(\text{DBTT}) = A \sum_i (\Delta g_b^{0i} - \Delta g_s^{0i}) \delta\Gamma^i \quad (35)$$

where the interpretation of A is

$$A = \frac{-\partial F/\partial(2\gamma_{\text{int}})}{1 + 2s_{\text{int}} \partial F/\partial(2\gamma_{\text{int}})} \quad (36)$$

Comparison with (31) then shows that the hypothesis is supported if the embrittlement sensitivities from fracture tests and the segregation energies from adsorption studies satisfy

$$\xi_i = A(\Delta g_b^{0i} - \Delta g_s^{0i}) \quad (37)$$

with the same coefficient A for every segregating chemical species i .

Since temper embrittlement of alloy steels by impurity segregation is an important, widely

studied, embrittlement phenomena, data for embrittlement sensitivities for steels (and otherwise "pure" iron) are available in the literature. Early data on embrittlement sensitivities of impurities in steels were summarized by Seah [68, 69] in terms of Kelvins per ppm by mass of the solute concentration in the bulk. These data are irrelevant to our comparison since they are not based on grain boundary coverage. As quantitative AES advanced in recent years measurements of the interfacial concentration of impurities became possible. Embrittlement sensitivities are typically reported in units of Kelvins per atomic % of solute coverage on grain boundaries. They are available for several detrimental impurities in steels, including phosphorus, tin, antimony and sulphur for which there are segregation energy data (Tables 1 and 2) and also for the important element carbon. Published values are listed in Table 3. The available data spread widely. As we pointed out previously, the shift of the ductile-brittle transition temperature, measured by standard Charpy impact tests, is not only dependent on the grain boundary segregation, but also a function of the resistance of the steel to plastic flow, which is determined by microstructure. Comparisons between different steels or for the same steel under different conditions are inappropriate. The most strictly comparable data are those for 3.5Ni-1.7Cr steels after heat treatments to obtain the same grain size and hardness. However, as we see from the table, data for this steel obtained by different research groups are

TABLE 3 Embrittlement sensitivities for steels (in K/at.% in g.b.)

Impurity	System	ξ	Reference
P	low-alloy steel	5.4	Guttman [63]
	12%Cr-Ni-Mo	6.0	Guillou <i>et al.</i> [70]
	34CrMo4	6.7	Erhart <i>et al.</i> [51]
	16MCND6	5.9	Guttman [71]
	16NC6	7.3	Guttman [71]
	Z12CND12	7.6	Guttman [71]
	3.5Ni-1.7Cr steel	16	McMahon <i>et al.</i> [72]
	Fe-P-C	10	Guttman [66]
Sn	3.5Ni-1.7Cr steel	20	Suzuki <i>et al.</i> [46, 54]
		38	McMahon <i>et al.</i> [72]
Sb	3.5Ni-1.7Cr steel	15	Guttman [66]
		67	McMahon <i>et al.</i> [72]
S	3.5Ni-1.7Cr steel	28	Guttman [66]
		40	Suzuki <i>et al.</i> [47]
C	Fe-S-C	40	Suzuki <i>et al.</i> [47]
	Fe-P-C	-10	Suzuki <i>et al.</i> [47]
		-20	Suzuki <i>et al.</i> [46, 54]

still scattered widely, probably owing to the difference in experimental conditions and calibration procedures for converting the Auger peak height ratio to the fracture surface coverage.

Ranges for the embrittlement sensitivities ξ_i , based on Table 3, have been summarized in the last column of Table 2. The plot of the ranges for the ξ_i against those for $(\Delta g_b^{0i} - \Delta g_s^{0i})$ at 300 K, also from Table 2, are shown in Fig. 8. These ranges are based on the values reported in different studies (often as few as two, defining the upper and lower limit to a range), and on other consideration as we have discussed, but include no account of uncertainties, or error bars, in any individual study. Thus, for example, we cannot at this point be certain that correct values for the ξ and $\Delta g_b^0 - \Delta g_s^0$ actually fall within the box shown for each segregant.

If there were none of the uncertainties or ambiguities mentioned in the values for the ξ_i and $\Delta g_b^{0i} - \Delta g_s^{0i}$, then the hypothesis could be judged as being supported if the data points fell approximately on a straight line, and not supported if otherwise. In the present situation there is little to conclude from Fig. 8. The trend for the detrimental segregants phosphorus, tin, antimony and sulphur cannot be judged as contradicting the hypothesis, given present uncertainties.

The straight line in Fig. 8 corresponds to $A = 0.37 \text{ (K/at.\% on g.b.)}/(\text{kJ mol}^{-1}) = 1400 \text{ K}/(\text{J m}^{-2})$ in (37). Thus, from (36) if we assume $2s_{\text{int}} = (0.5 \text{ to } 1.0) \times 10^{-3} \text{ J m}^{-2} \text{ K}^{-1}$ [74, 75], that straight line implies

$$\partial F/\partial(2\gamma_{\text{int}}) \approx -(580 \text{ to } 820) \text{ K}/(\text{J m}^{-2}) \quad (38)$$

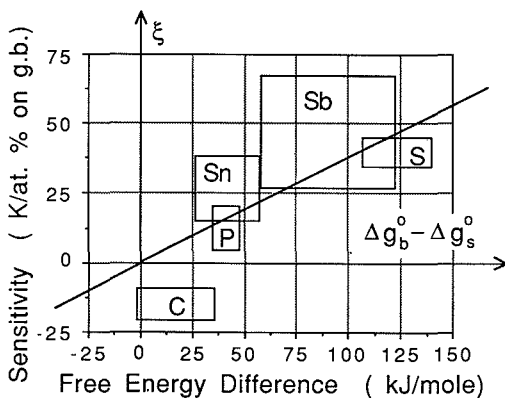


Fig. 8. Plot of approximate ranges for embrittlement sensitivities, ξ , against approximate ranges for difference in free energy of segregation, $\Delta g_b^0 - \Delta g_s^0$. See Tables 1-3 and text for discussion of data.

That is, each 0.1 J m^{-2} reduction in $2\gamma_{\text{int}}$ due to segregation of solutes such as phosphorus, tin, antimony or sulphur increases the DBTT by the order of 60 to 80 K.

Results for carbon in Fig. 8 are inconsistent with the trend of the other segregants. The $\Delta g_b^0 - \Delta g_s^0$ range that we give for carbon suggests that it is a mildly embrittling element. Such is not inconsistent with the net effect of carbon being beneficial, because it also displaces worse embrittlors from grain boundaries by site competition. However, there is evidence that after accounting for displacement effects, there is an additional effect of carbon as a cohesion enhancer (see for example refs. 46 and 54), signified by the negative ξ in Tables 2 and 3. This may mean that effects of carbon segregation on embrittlement cannot be understood in terms of an alteration of $2\gamma_{\text{int}}$. It is, nevertheless, well to remember that we have had to use the (100) crystal surface segregation energy for carbon, in absence of results for carbon adsorption on polycrystal surfaces created by intergranular fracture. As remarked, this may result in our reported range for $\Delta g_b^0 - \Delta g_s^0$ being a significant overestimate. The possibility cannot presently be ruled out that a more appropriate, polycrystalline range of $\Delta g_b^0 - \Delta g_s^0$ for carbon would be negative, in better agreement with the trend of proportionality of the ξ to the $\Delta g_b^0 - \Delta g_s^0$ that is required when $2\gamma_{\text{int}}$ controls embrittlement.

6. Summarizing remarks

We have reviewed theoretical models of intergranular fracture with an emphasis on understanding effects of solute segregation on the process. Of parameters susceptible to alteration by solute segregation, the models point to an important role for alterations of $2\gamma_{\text{int}}$, the ideal work of separation of an interface, in governing embrittlement. Nevertheless, alterations of the peak strength σ_{max} , the shape of the σ vs. δ relation and of other potentials for the interfacial region, and of poorly understood parameters characterizing dislocation generation at, and mobility through, the interface may also be important for embrittlement.

A thermodynamic framework is outlined which allows results of solute adsorption studies for grain boundaries and free surfaces to be used to estimate alterations in $2\gamma_{\text{int}}$ due to solute segregation. For light, sub-monolayer coverage, the

critical parameter giving the decrease of $2\gamma_{\text{int}}$ per unit increase of solute coverage is $\Delta g_{\text{b}}^0 - \Delta g_{\text{s}}^0$. This is the difference in the (inherently negative) free energies of segregation from the bulk to a grain boundary and from the bulk to a free surface. That is, it is the reversible work of moving a solute atom from a specific adsorption site along a free surface to a specific site along a grain boundary.

For the special case of dilute temper embrittling solutes in steels, or iron, we summarize data giving approximate ranges of the free energy difference. This can be done, with various uncertainties, for carbon, phosphorus, tin, antimony and sulphur.

The effects of such solute segregation on shifting the DBTT in the Charpy impact test has been summarized in terms of embrittlement sensitivities ξ . Values have been summarized here from the literature. We show that the hypothesis that embrittlement can be understood solely in terms of the effects of solute segregation on $2\gamma_{\text{int}}$ requires that the ratio of ξ to $\Delta g_{\text{b}}^0 - \Delta g_{\text{s}}^0$ be the same for every segregant. We attempt to use the available data to test the hypothesis, but the uncertainties in the data are too great to allow any sharp conclusions. Results for the detrimental segregants, phosphorus, tin, antimony and sulphur may plausibly support the hypothesis, but not those that we show for carbon. This may be either because carbon's effects (beyond those due to its displacement of deleterious segregants through site competition) are not explicable in terms of the effect of carbon segregation on $2\gamma_{\text{int}}$, or because the surface segregation energy that we have used in the correlation, available only for carbon on (100) surfaces, overestimates the magnitude of segregation energy for a polycrystal surface formed by intergranular fracture. If the latter is true, the hypothesis regarding $2\gamma_{\text{int}}$ may hold for carbon also.

It is unlikely that experimental techniques for study of surface and grain boundary adsorption will improve enough in the near future to significantly reduce the uncertainties that we have encountered. Possibly, first-principles quantum electronic calculations of the difference in bonding energies for a solute in a grain boundary and in a free surface environment will provide a quicker and more accurate route to understanding alterations of $2\gamma_{\text{int}}$ by solute segregation. Such calculations are encouraged and should also provide useful guidelines on what factors make

for large or small, positive or negative (i.e. cohesion enhancing), values of $\Delta g_{\text{b}}^0 - \Delta g_{\text{s}}^0$.

More definitive fracture experiments than those provided by the Charpy test would also be of great help in testing theoretical concepts. Ideally, one might measure the macroscopic fracture energy G for bicrystal specimens, for a fixed set of adjoining crystal orientations and with variable amounts and types of segregated solutes for each such orientation, and characterize the extent to which G correlates with $2\gamma_{\text{int}}$ or with other quantities susceptible to alteration by solute segregation.

Acknowledgments

This study was supported by the NSF Materials Research Laboratory at Harvard University, and by the University of California through subcontract to Harvard based on support by the Office of Naval Research contract N00014-86-K-0753. We are grateful to Greg Olson for helpful discussion.

References

- 1 M. Guttman and D. McLean, in W. C. Johnson and J. M. Blakely (eds.), *Interfacial Segregation*, ASM, Metals Park, OH, 1979, p. 261.
- 2 C. L. Briant and S. K. Banerji, in C. L. Briant and S. K. Banerji (eds.), *Embrittlement of Engineering Alloys*, Academic Press, New York, 1983, p. 21.
- 3 A. Fraczkiewicz and M. Biscondi, *J. Phys. Paris Colloq. C4*, 46 (1985) 497.
- 4 C. T. Liu, C. L. White and J. A. Horton, *Acta Metall.*, 33 (1985) 213.
- 5 C. L. White, *J. Vac. Sci. Technol. A*, 4 (1986) 1633.
- 6 B. R. Lawn and T. R. Wilshaw, *Fracture of Brittle Solids*, Cambridge University Press, Cambridge, 1975.
- 7 J. R. Rice, *J. Appl. Mech.*, 55 (1988) 98.
- 8 J. R. Rice, in R. M. Latanision and R. H. Jones (eds.), *Chemistry and Physics of Fracture*, Martinus Nijhoff, Dordrecht, 1987, p. 22.
- 9 J. R. Rice, in H. Liebowitz (ed.), *Fracture: An Advanced Treatise*, Vol. 2, Academic Press, New York, 1968, p. 191.
- 10 A. C. Palmer and J. R. Rice, *Proc. R. Soc. London Ser. A*, 332 (1973) 527.
- 11 J. H. Rose, J. R. Smith and J. Ferrante, *Phys. Rev. B*, 28 (1983) 1835.
- 12 J. H. Rose, J. R. Smith, F. Guinea and J. Ferrante, *Phys. Rev. B*, 29 (1984) 2963.
- 13 J. Ferrante and J. R. Smith, *Phys. Rev. B*, 31 (1985) 3427.
- 14 R. Thomson, in R. M. Latanision and J. Pickens (eds.), *Atomistics of Fracture*, Plenum, New York, 1983, p. 167.
- 15 R. Thomson, in H. Ehrenreich and D. Turnbull (eds.), *Solid State Physics*, Vol. 39, Academic Press, New York, 1986, p. 1.
- 16 D. M. Esterling, *J. Appl. Phys.*, 47 (1976) 486.

- 17 B. de Cellis, A. S. Argon and S. Yip, *J. Appl. Phys.*, 54 (1983) 4864.
- 18 J. R. Rice, in R. E. Kelly (ed.), *Proc. 8th U.S. Natl. Congr. on Applied Mechanics*, Western Periodicals, N. Hollywood, 1979, p. 191.
- 19 J. F. Knott, in R. M. Latanision and J. Pickens (eds.), *Atomistics of Fracture*, Plenum, New York, 1983, p. 209.
- 20 J. F. Knott, in R. M. Latanision and R. H. Jones (eds.), *Chemistry and Physics of Fracture*, Martinus Nijhoff, Dordrecht, 1987, p. 44.
- 21 J. R. Rice, *J. Mech. Phys. Solids*, 26 (1978) 61.
- 22 J. R. Rice, in A. W. Thompson and I. M. Bernstein (eds.), *Effect of Hydrogen on Behavior of Materials*, The Metallurgical Society of AIME, Warrendale, PA, 1976, p. 455.
- 23 D. D. Mason, *Philos. Mag.*, 39 (1979) 455.
- 24 M. P. Seah and D. Hondros, in R. M. Latanision and J. Pickens (eds.), *Atomistics of Fracture*, Plenum, New York, 1983, p. 855.
- 25 P. M. Anderson and J. R. Rice, *Scr. Metall.*, 20 (1986) 1467.
- 26 J.-S. Wang, P. M. Anderson and J. R. Rice, in M. G. Yan, S. H. Zhang and Z. M. Zheng (eds.), *Mechanical Behavior of Materials—V*, Pergamon, Oxford, 1987, p. 191.
- 27 J. Yu and J. R. Rice, in M. H. Yoo, C. L. Briant and W. A. T. Clark (eds.), *Interfacial Structure, Properties and Design*, Materials Research Society, Vol. 122, 1988, in press.
- 28 L. B. Freund and J. W. Hutchinson, *J. Mech. Phys. Solids*, 33 (1985) 169.
- 29 J. P. Hirth and J. Lothe, *Theory of Dislocations* (Appendix 2), McGraw-Hill, New York, 1968.
- 30 J. S. Wang, in M. H. Yoo, C. L. Briant and W. A. T. Clark (eds.), *Interfacial Structure, Properties and Design*, Materials Research Society, Vol. 122, 1988, in press.
- 31 M. L. Jokl, V. Vitek and C. J. McMahon, Jr., *Acta Metall.*, 28 (1980) 1479.
- 32 E. W. Hart, *Int. J. Solids Struct.*, 16 (1980) 807.
- 33 C. Y. Hui and H. Riedel, *Int. J. Fracture*, 17 (1981) 409.
- 34 K. K. Lo, *J. Mech. Phys. Solids*, 31 (1983) 287.
- 35 P. A. Mataga, L. B. Freund and J. W. Hutchinson, *J. Phys. Chem. Solids*, 48 (1987) 985.
- 36 J. R. Rice and M. A. Johnson, in M. F. Kanninen, W. F. Adler, A. R. Rosenfield and R. I. Jaffee (eds.), *Inelastic Behavior of Solids*, McGraw-Hill, New York, 1970, p. 641.
- 37 A. Needleman, submitted to *Int. J. Fracture*.
- 38 J. P. Hirth and J. R. Rice, *Metall. Trans. A*, 11 (1980) 1502.
- 39 R. J. Asaro, *Phil. Trans. R. Soc. London Ser. A*, 295 (1980) 150.
- 40 M. E. Eberhart, K. H. Johnson, R. P. Messner and C. L. Briant, in R. M. Latanision and J. Pickens (eds.), *Atomistics of Fracture*, Plenum, New York, 1983, p. 255.
- 41 D. McLean, *Grain Boundaries in Metals*, Oxford University Press, Oxford, 1957.
- 42 E. D. Hondros and M. P. Seah, *Metall. Trans. A*, 8 (1977) 1363.
- 43 H. Hänsel and H. J. Grabke, *Scr. Metall.*, 20 (1986) 1641.
- 44 H. Kimura, K. Abiko, S. Suzuki, M. Obata, J.-I. Kumagai and H. Kimura, in *Grain Boundary Structure and Related Phenomena*, Proc. JIMIS-4, 1986, p. 53.
- 45 H. Kimura, K. Abiko and S. Suzuki, in M. H. Yoo, C. L. Briant and W. A. T. Clark (eds.), *Interfacial Structure, Properties and Design*, Materials Research Society, Vol. 122, 1988, in press.
- 46 S. Suzuki, M. Obata, K. Abiko and H. Kamura, *Trans. Iron Steel Inst. Jpn.*, 25 (1985) 62.
- 47 S. Suzuki, S. Tani, K. Abiko and H. Kimura, *Metall. Trans. A*, 18 (1987) 1109.
- 48 K. Abiko, S. Suzuki and H. Kimura, *Trans. Jpn. Inst. Metals*, 23 (1982) 43.
- 49 R. Möller and H. J. Grabke, *Scr. Metall.*, 18 (1984) 527.
- 50 H. Erhart and H. J. Grabke, *Metall. Sci.*, 15 (1981) 401.
- 51 H. Erhart, H. J. Grabke and R. Möller, *Arch. Eisenhüttenwes*, 52 (1981) 451.
- 52 M. Guttman, Ph. Dumoulin and M. Wayman, *Metall. Trans. A*, 13 (1982) 1693.
- 53 Y. E. Glickman, V. F. Kotyshev, Y. L. Cherpakov and R. E. Bruver, *Phys. Met. Metallogr. (U.S.S.R.)*, 36 (1973) 126.
- 54 S. Suzuki, M. Obata, K. Abiko and H. Kimura, *Scr. Metall.*, 17 (1983) 1325.
- 55 H. J. Grabke, in R. M. Latanision and R. H. Jones (eds.), *Chemistry and Physics of Fracture*, Martinus Nijhoff, Dordrecht, 1987, p. 388.
- 56 H. J. Grabke, *Steel Research*, 57 (1986) 178.
- 57 G. Tauber and H. J. Grabke, *Ber. Bunsenges Phys. Chem.*, 82 (1978) 298.
- 58 K. S. Shin and B. H. Tsao, *Scr. Metall.*, 22 (1988) 585.
- 59 M. Rußenberg and H. Viehhaus, *Surf. Sci.*, 159 (1985) 1.
- 60 H. J. Grabke, W. Pualitschke, G. Tauber and H. Viehhaus, *Surf. Sci.*, 63 (1977) 377.
- 61 M. P. Seah and C. Lea, *Philos. Mag.*, 31 (1975) 627.
- 62 C. Lea and M. P. Seah, *Surf. Sci.*, 53 (1975) 273.
- 63 M. Guttman, in R. M. Latanision and J. R. Pickens (eds.), *Atomistics of Fracture*, Plenum, New York, 1983, p. 465.
- 64 Ph. Dumoulin and M. Guttman, *Mater. Sci. Eng.*, 42 (1980) 249.
- 65 J. M. Papazian and D. N. Beshers, *Metall. Trans.*, 2 (1971) 491.
- 66 M. Guttman, *Phil. Trans. R. Soc. London Ser. A*, 295 (1980) 169.
- 67 M. Guttman, *Surf. Sci.*, 53 (1975) 168.
- 68 M. P. Seah, *Surf. Sci.*, 53 (1975) 213.
- 69 M. P. Seah, *Proc. R. Soc. London Ser. A*, 349 (1976) 535.
- 70 R. Guillou, M. Guttman and Ph. Dumoulin, *Metal Sci.*, 15 (1981) 63.
- 71 M. Guttman, in R. M. Latanision and R. J. Courtney (eds.), *Advances in the Mechanics and Physics of Surfaces*, Vol. 1, Harwood Academic Publishers, Chur., 1981, p. 1.
- 72 C. J. McMahon, Jr. and L. Marchut, *J. Vac. Sci. Technol.*, 15 (1978) 450.
- 73 M. Guttman, *Mater. Sci. Eng.*, 42 (1980) 227.
- 74 W. R. Tyson, *Can. Metall. Q.*, 14 (1975) 307.
- 75 L. E. Murr, *Interface Phenomena in Metals and Alloys*, Addison-Wesley, Boston, MA, 1975.